The two Ru-O distances are nearly identical [2.106 (3), 2.107 (3) Å] and only slightly shorter than the Os-O distances in the Os analogue [2.118 (6) Å]. The Ru-O distances compare well with Ru-O distances observed in some dinuclear Ru species having similar groups.[37] Altogether, the bond length distribution in **1** conforms well to the molecular quasi *m* symmetry (the pseudo-mirror plane passing through Ru(2) and the midpoint of the Ru(1)-Ru(3) bond). Such molecular symmetry is in fact broken only by the Si-Et group orientations.

Implications for Surface Organometallic Chemistry. Interaction of the silanol and silanolate derivatives with the triruthenium clusters in the absence of catalytic amounts of $Cp_2Fe_2(CO)_4$ resembles the reactivity pattern encountered upon chemisorption of $Ru_3(CO)_{12}$ on the basic MgO support, in which exlusively reduction products are observed. In contrast, oxidative addition of a surface silanol group to the metal-metal bond of $Ru_3(CO)_{12}$ occurs upon chemisorption of the trinuclear cluster on silica. Although the different reactivity patterns are probably a consequence of the intrinsic properties of the SiO_2 surface, the oxidative addition pathway may require activation of a carbonyl ligand in a manner similar to that proposed for the catalytic action of the iron dimer.

The synthesis of **1** was made possible by the presence of catalytic amounts of $Cp_2Fe_2(CO)_4$. This result suggests that a similar approach may be a viable alternative for incorporating species within the coordination sphere of a metal cluster, which tends to yield reduction products exclusively.

Acknowledgment. We are grateful to Dr. A. L. Rheingold of the University of Delaware for the determination of the unit cell parameters for $H_2Ru_4(CO)_{13}$ and $H_2Ru_6(CO)_{18}$. This work was supported by the National Science Foundation (Grants CBT-8605699, CHE 86-02941, and CHE 87-01413).

Supplementary Material Available: Tables of crystal data, anisotropic thermal parameters, fractional atomic coordinates and thermal parameters, fractional atomic coordinates and thermal parameters for the hydrogen atoms, and complete bond distances and angles (27 pages); F_o/F_c tables (20 pages). Ordering information is given on any current masthead page.

Contribution from the Department of Chemistry, Washington State University, Pullman, Washington 99164-4630

Solvent, Anion, and Temperature Dependences of the Ruthenocene(II)/Bromoruthenocene(IV) and Ruthenocene(II)/Iodoruthenocene(IV) Electron Exchange

Karl Kirchner, Harold W. Dodgen, Scot Wherland, and John P. Hunt*

Received May 1, 1989

The rates of the electron exchange between $Ru(cp)_2$ and $Ru(cp)_2Br^+$ (cp represents the cyclopentadienide anion) as the PF_6^-, ClO_4^-, and BF_4^- salts and between $Ru(cp)_2$ and $Ru(cp)_2I^+$ as the $CF_3SO_3^-$ and PF_6^- salts have been measured by ^1H NMR line broadening as a function of temperature and solvent. The observed second-order rate constants at 20 °C and the activation parameters obtained for the $Ru(cp)_2/Ru(cp)_2Br^+$ system as the PF_6^- salt are as follows ($10^{-3}k$ in M^{-1} s^{-1}, ΔH^* in kcal mol^{-1}, ΔS^* in cal mol^{-1} K^{-1}): nitrobenzene-d_5, 2.9 ± 0.2, 8.1 ± 0.1, −14.8 ± 0.2; nitromethane-d_3, 2.5 ± 0.1, 8.5 ± 0.1, −14.1 ± 0.5; acetonitrile-d_3, 1.6 ± 0.08, 8.2 ± 0.1, −15.7 ± 0.3; benzonitrile, 1.6 ± 0.08, 8.6 ± 0.3, −14.5 ± 1.1. For the $Ru(cp)_2/Ru(cp)_2I^+$ system as the $CF_3SO_3^-$ salt, the second-order rate constants at 20 °C and the activation parameters obtained are as follows ($10^{-5}k$ in M^{-1} s^{-1}, ΔH^* in kcal mol^{-1}, ΔS^* in cal mol^{-1} K^{-1}): nitrobenzene-d_5, 2.6 ± 0.1, 6.6 ± 0.1, −11.3 ± 0.3; nitromethane-d_3, 19.2 ± 1.0, 8.5 ± 0.3, −0.5 ± 0.7; acetonitrile-d_3, 7.4 ± 0.4, 6.7 ± 0.2, −8.7 ± 0.8. Only a slight dependence on extra added salt is found for the above solvents. In the low dielectric constant solvents, chloroform-d_1, bromobenzene-d_5, and methylene-d_2 chloride, ion association occurs and thus the observed rate constants and activation parameters are composite quantities from free-ion and ion-paired pathways. For chloroform-d_1, the rate constants for two pathways are resolved. The calculations indicate that the electron-transfer reaction does not occur appreciably via the ion-paired pathway. There is no significant dependence of rate on the identity of the counterion. Decamethylruthenocene(II) does not exchange with bromo- or iododecamethylruthenocene(IV) even at 110 °C in nitrobenzene-d_5.

Introduction

The study of one-electron-transfer reactions between substitution-inert monometallic transition-metal complexes in nonaqueous solution has become an appealing area of research in recent years. Consequently, considerable progress has been made in both experimental and theoretical respects.[1-3] However, reports on multielectron-transfer reactions between monometallic transition-metal complexes are sparse.[4] A prototypical example of a simple two-electron, apparently inner-sphere, exchange reaction was introduced by Taube et al., namely the halogen-mediated electron transfer between metallocenes of ruthenium and osmium in the oxidation states 4+ and 2+.[5] The reactants are stable in both oxidation states in solution over a large range of temperatures and pressures. A comparison of solvent electrolyte effects between inner-sphere and outer-sphere electron-exchange reactions might be of interest.

In these two-electron-transfer reactions, structural changes that accompany charge transfer and the activation process will be in contrast with those of simple outer-sphere self-exchange reactions. Variation of solvent, temperature, electrolyte, and anion may give a deeper insight into the detailed mechanism of this reaction type. Other important questions concerning two-electron transfers are how the halogen exerts control on the reaction, whether a concerted two-electron process occurs or whether two one-electron steps are involved, and if the latter occurs, whether Ru(III) intermediates can be detected.

In this paper we report an investigation of the kinetics for various temperatures, solvents, and anions for the ruthenocene/bromoruthenocene and ruthenocene/iodoruthenocene electron-exchange reactions.

Experimental Section

Materials. Ruthenocene was obtained from Strem Chemicals, Inc., and was purified by one vacuum sublimation. $[Ru(cp)_2Br]X$ (X = PF_6^-, BF_4^-, ClO_4^-) and $[Ru(bp)_2I]X$ (X = $CF_3SO_3^-$, PF_6^-) were synthesized according to refs 6 and 7. $[Ru(cp)_2Br]X$ was recrystallized twice from

(1) Cannon, R. D. *Electron Transfer Reactions*; Butterworth: London, 1980.
(2) Sutin, N. *Acc. Chem. Res.* **1982**, *15*, 275.
(3) Sutin, N. *Prog. Inorg. Chem.* **1983**, *30*, 441.
(4) Finke, R. G.; Voegeli, R. H.; Laganis, E. D.; Boekelheide, V. *Organometallics* **1983**, *2*, 347.
(5) Smith, T. P.; Iverson, D. J.; Droege, M. W.; Kwan, K. S.; Taube, H. *Inorg. Chem.* **1987**, *26*, 2882.
(6) Smith, T. P.; Kwan, K. S.; Taube, H.; Bino, A.; Cohen, S. *Inorg. Chem.* **1984**, *23*, 1943.
(7) Sohn, Y. S.; Schlueter, A. W.; Hendrickson, D. N.; Gray, H. B. *Inorg. Chem.* **1974**, *13*, 301.

0020-1669/90/1329-2381$02.50/0

hot acetonitrile/methylene chloride and precipitated with increments of *n*-heptane over a period of 1 h. Attempts to synthesize the triflate salt in the same manner were not successful. Anal. Calcd for $[C_{10}H_{10}BrRu]PF_6$: C, 26.33; H, 2.21. Found: C, 26.25; H, 2.41. Calcd for $[C_{10}H_{10}BrRu]BF_4$: C, 29.91; H, 2.51. Found: C, 30.13; H, 2.71. Calcd for $[C_{10}H_{10}BrRu]ClO_4$: C, 29.25; H, 2.45. Found: C, 29.84; H, 2.36. $[Ru(cp)_2I]X$ was purified as in ref 6. Anal. Calcd for $[C_{10}H_{10}IRu]CF_3SO_3$: C, 26.05; H, 1.98; S, 6.32; I, 25.02. Found: C, 26.06; H, 1.98; S, 6.32; I, 25.02. Microanalyses were done by Galbraith Laboratories. Decamethylruthenocene was purchased from Strem Chemicals, Inc., and used without further purification. The corresponding haloruthenocene(IV) complexes were synthesized and purified according to a literature method.[6] All solvents used for the purification of both compounds were purchased from J. T. Baker Chemicals and purified by using standard procedures.[8] The deuterated solvents were purchased from MSD Isotopes and were used as obtained.

In the kinetics experiments the concentration of the reactants varied from about 0.5 to 20 mM depending on solubility.

^{1}H NMR Experiments. The data were recorded on a Nicolet N-T200WB instrument operating at 200 MHz. The acquisition parameters were a 4.5-μs pulse with a 500-ms postacquisition delay, a 2000-Hz sweep width, an 8K or 16K block size, and 256–1024 pulses. for the nondeuterated solvents no lock was used but after 64 scans a good signal-to-noise ratio was obtained. Temperature was controlled within ±1 °C by using the built-in gas-flow temperature controller. Temperature readings were calibrated against the temperature dependence of the proton chemical shifts of acidified methanol or ethylene glycol. The digitized data were transferred to an 80286 processor-based microcomputer running Microsoft Quick Basic and treated by a complete line shape analysis to obtain the second-order electron-exchange rate constants. The spectra were calculated by using a modified Bloch equation for two exchanging sites.[9,10] The nonlinear least-squares program allows the adjustment of the first-order exchange rate constant k' and/or the fraction of Ru(IV) complex by minimizing reduced χ^2. With this procedure it was possible to determine k' within an error of ±5% or better. Assuming a simple bimolecular rate law, the second-order exchange rate constant, k, is then given by $k'/[Ru(IV)]$. For the $Ru(cp)_2/Ru(cp)_2Br^+$ system in benzonitrile and for the $Ru(cp)_2/Ru(cp)_2I^+$ system in chloroform-d_1, methylene-d_2 chloride, and bromobenzene-d_5, second-order rate constants were extracted by using relations 1a,b, which were applicable since the reaction

$$k = \frac{\pi(\Delta\nu_{ex}^{II} - \Delta\nu_0^{II})}{[Ru(IV)]} \quad (1a)$$

$$k = \frac{\pi(\Delta\nu_{ex}^{IV} - \Delta\nu_0^{IV})}{[Ru(II)]} \quad (1b)$$

was in the slow-exchange regime, as indicated by obeying the relation $1/k' \gg 1/[2\pi(\delta\nu)]$. $\delta\nu$ is the difference of the resonance frequency (in Hz) of the Ru(II) and Ru(IV) complexes. In these equations k is the second-order rate constant, $\Delta\nu_{ex}^{II}$ and $\Delta\nu_{ex}^{IV}$ are the full widths at half-height of Ru(II) and Ru(IV) in Hz in the presence of Ru(IV) and Ru(II), respectively, and $\Delta\nu_0^{II}$ and $\Delta\nu_0^{IV}$ are the full widths at half-height in Hz of Ru(II) and Ru(IV) in the absence of Ru(IV) and Ru(II), respectively. The peak widths at half-height were determined by fitting the data to a Lorentzian line shape using the program LF available on the Nicolet instrument. NMR line widths and chemical shifts, relative to tetramethylsilane (TMS), for the pure compounds were measured in all solvents at various temperatures.

The temperature dependence data were fit to the Eyring equation by using a simple linear least-squares program. The errors were derived from the scatter of k about the fit lines.

Conductivity Experiments. Conductivity experiments were run at the Technical University of Vienna in a thermostated cell with a cell constant of 0.43 cm^{-1}. The cell constant was measured by using aqueous KCl solutions. Cell resistance was measured with a Wayne Kerr Autobalance Universal Bridge B 642 using a Pt electrode at 25 ± 0.1 °C.

Results

The proton NMR spectra of $Ru(cp)_2$ and $Ru(cp)_2Br^+$ (PF_6^-, BF_4^-, and ClO_4^- as counterions) show a single line at δ = 4.53 ppm and δ = 6.07 ppm vs TMS, respectively, in the solvents acetonitrile-d_3, nitromethane-d_3, methylene-d_2 chloride, and benzonitrile. In nitrobenzene-d_5 for $Ru(cp)_2Br^+$ δ = 6.26 ppm was found. The full line widths at half-height of $Ru(cp)_2$ and $Ru(cp)_2Br^+$ are 0.2 ± 0.02 Hz. The chemical shifts and the line widths are independent of temperature. The kinetic results of the temperature and solvent dependences are summarized in Table I and shown in Figure 1.

$Ru(cp)_2I^+$ (PF_6^- and $CF_3SO_3^-$ as counterions) exhibits a single resonance at δ = 6.07 ppm in the solvents acetonitrile-d_3 and nitromethane-d_3. In chloroform-d_1, methylene-d_2 chloride, nitrobenzene-d_5, and bromobenzene-d_5 the single peak is shifted to δ = 6.27, 6.15, 6.30, and 5.61 ppm, respectively. The line width in these solvents is 0.2 ± 0.1 Hz. Both the line widths and the chemical shifts are independent of temperature in the range studied.

Care was taken to avoid use for the kinetic studies of some batches of $[Ru(cp)_2I]CF_3SO_3$, for which, particularly in low dielectric solvents, the line widths were significantly broadened as the temperature increased from −10 °C. However, no broadening of other signals, e.g. of TMS or solvent, was observed and no additional peaks due to decomposition could be detected. The profile of shift versus temperature plots was reproducible for the same solutions as the temperature increased and decreased. This indicates reversibility of the underlying processes. Just a slight increase of the widths at lower temperatures was observed. The ratios of the peak areas of the $Ru(cp)_2I^+$ signal and the solvent or TMS signals were independent of temperature within the time scale of the measurements. After addition of small amounts of iodine as an oxidant to a solution of iodoruthenocene(IV), no temperature-dependent broadening was observed and the line

Table I. Activation Parameters and Observed Second-Order Rate Constants at 20 °C for the $Ru(cp)_2/[Ru(cp)_2Br]PF_6$ System in Various Solvents

solvent (ϵ)	no. of pts	T range (±1), °C	$\Delta H^{\ddagger}$, kcal mol^{-1}	$\Delta S^{\ddagger}$, cal mol^{-1} K^{-1}	$10^{-3}k$,[a] M^{-1} s^{-1}
CD_3CN (37.5)	6	20–70	8.2 ± 0.1	−15.7 ± 0.3	1.6[d]
CD_3NO_2 (35.8)	5	20–60	8.5 ± 0.1	−14.1 ± 0.5	2.5[d]
$C_6D_5NO_2$ (34.8)	16	20–110	8.1 ± 0.1	−14.8 ± 0.2	2.9[d]
C_6H_5CN (25.2)	12	20–45	8.6 ± 0.3	−14.5 ± 1.1	1.6[d]
CD_2Cl_2 (8.9)	11	5–35	6.0 ± 0.1	−17.8 ± 0.4	25.2[e]
CD_3CN[b]	6	20–70	8.5 ± 0.2	−14.9 ± 0.3	1.7
CD_3CN[c]	6	20–70	8.4 ± 0.2	−15.2 ± 0.2	1.7

[a] Assumed second-order rate law; see text. [b] ClO_4^- as anion. [c] BF_4^- as anion. [d] Concentration range of $[Ru(cp)_2Br]PF_6$: 9.9–19.1 mM. [e] Concentration range of $[Ru(cp)_2Br]PF_6$: 0.52–0.56 mM.

Table II. Activation Parameters and Observed Second-Order Rate Constants at 20 °C for the $Ru(cp)_2/[Ru(cp)_2I]CF_3SO_3$ System in Various Solvents

solvent (ϵ)	no. of pts	T range (±1), °C	$\Delta H^{\ddagger}$, kcal mol^{-1}	$\Delta S^{\ddagger}$, cal mol^{-1} K^{-1}	$10^{-5}k$,[a] M^{-1} s^{-1}
CD_3CN (37.5)	17	−30–20	6.7 ± 0.2	−8.7 ± 0.8	7.4[b]
CD_3NO_2 (35.8)	14	−10–35	8.5 ± 0.3	−0.5 ± 0.7	19.2[b]
$C_6D_5NO_2$ (34.8)	16	15–80	6.6 ± 0.1	−11.3 ± 0.3	2.6[b]
CD_2Cl_2 (8.9)	32	−90 to −50	5.7 ± 0.1	−12.9 ± 0.7	5.4[c]
$CDCl_3$ (4.7)	48	−60–30	1.9 ± 0.1	−33.8 ± 0.4	0.086[b]
C_6D_5Br (5.4)	16	−20–50	5.3 ± 0.2	−23.9 ± 0.6	0.037[b]

[a] Assumed second-order rate law; see text. [b] In the slow-exchange regime the rate constants were determined by using both broadenings of the Ru(II) and Ru(IV) signals according to eq 1. An average value is given. [c] Extrapolated to 20 °C.

Table III. Activation Parameters and Observed Second-Order Rate Constants at 20 °C for the $Ru(cp)_2/[Ru(cp)_2I]PF_6$ System in Various Solvents

solvent (ϵ)	no. of pts	T range (±1), °C	$\Delta H^{\ddagger}$, kcal mol^{-1}	$\Delta S^{\ddagger}$, cal mol^{-1} K^{-1}	$10^{-5}k$,[a] M^{-1} s^{-1}
CD_3CN (37.5)	13	−30–25	6.2 ± 0.2	−8.3 ± 0.8	21.1[b]
CD_3NO_2 (35.8)	9	−10–30	8.7 ± 0.2	−0.3 ± 0.6	19.1
CD_2Cl_2 (8.9)	10	−85 to −65	5.2 ± 0.2	−12.6 ± 0.8	14.3[c]

[a] Assumed second-order rate law; see text. [b] In the slow-exchange regime the rate constants were determined by using both broadenings of the Ru(II) and Ru(IV) signals according to eq 1. An average value is given. [c] Extrapolated to 20 °C.

(8) Riddick, J. A.; Bunger, W. B. *Organic Solvents: Physical Properties and Methods of Purification*, 3rd ed.; Wiley: New York, 1970.
(9) Pople, J. A.; Schneider, N. G.; Bernstein, H. J. *High Resolution Nuclear Magnetic Resonance*; McGraw-Hill Book Co., Inc.: New York, 1958.
(10) Anderson, K.; Wherland, S. *Inorg. Chem.* **1989**, *28*, 601.

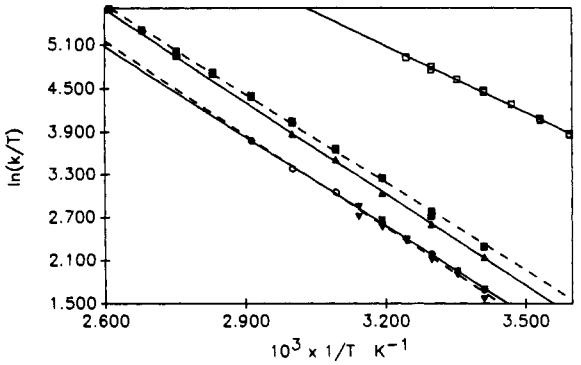

Figure 1. Eyring plots for the $Ru(cp)_2/[Ru(cp)_2Br]PF_6$ electron exchange in different solvents: (○) CD_3CN (solid line); (▼) C_6H_5CN (dashed line); (▲) CD_3NO_2 (solid line); (■) $C_6D_5NO_2$ (dashed line); (□) CD_2Cl_2.

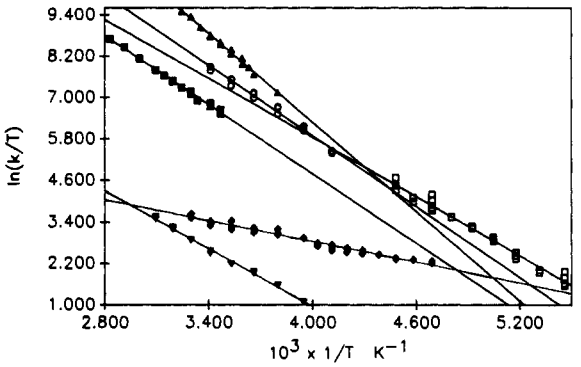

Figure 2. Eyring plots for the $Ru(cp)_2/[Ru(cp)_2I]CF_3SO_3$ electron exchange in different solvents: (○) CD_3CN; (▲) CD_3NO_2; (■) $C_6D_5NO_2$; (□) CD_2Cl_2; (♦) $CDCl_3$; (▽) C_6D_5Br.

width at half-height was about 0.2 Hz.

Due to overlap between the solute and the solvent signal in methylene-d_2 chloride, the electron self-exchange was studied only between −90 and −50 °C. The results of these kinetic studies are shown in Figure 2 and summarized in Tables II and III. The choice of different solvents was limited by the solubility and the stability of the haloruthenocene(IV) complexes as pointed out in a previous paper.[11]

It was found that the decamethyl derivatives of ruthenocene(II) and both bromo- and iodoruthenocene(IV) complexes do not undergo exchange even at 110 °C in nitrobenzene-d_5. An upper limit of k, based on the resolution of the NMR spectrometer due to the field inhomogeneity (≤0.2 Hz) and on the solubility of the complexes (20 to 30 mM in nitrobenzene-d_5), can be estimated to be ca. 25 ± 5 M^{-1} s^{-1}. At higher temperatures decomposition occurred and precluded extending the temperature range.

For the $Ru(cp)_2/Ru(cp)_2I^+$ system the rate was studied as a function of concentration in the solvents acetonitrile-d_3 at −30 °C, methylene-d_2 chloride at −50 °C, and chloroform-d_1 at −20 and 20 °C. The low solubility of iodoruthenocene in bromobenzene did not permit a concentration dependence study in this solvent. As a representative example, the concentration dependence in chloroform-d_1 at 20 °C is shown in Table IV. In acetonitrile-d_3 the rate constants do not appreciably change when reactant concentrations are varied and the second-order rate law is valid. However, in the low dielectric constant solvents the overall rate constant increases as the concentration of $Ru(cp)_2I^+$ decreases. There is no effect on the rate constants of changing the $Ru(cp)_2$ concentration.

The conductance data were fit by means of a nonlinear least-squares program, minimizing χ^2, to both Fuoss–Kraus[12] and Fuoss–Hsia[13] equations. The latter one was used in the form presented by Fernandez-Prini.[14] As suggested by Beronius,[15] only the molar limiting conductance, λ_0, and the ion-pair formation constant, $K_{ip}°$, were treated as adjustable parameters. The distance parameter, r, was optimized by setting it equal to a number of values. The best value for r was determined by plotting χ^2 versus r. The results of fitting the conductivity data over the concentration range 0.02–0.5 mM at 25 °C are given in Table V. The two different equations used for the evaluation of the molar limiting conductance and the association constant gave similar results. In the equations of Fuoss and Hsia, where the extended Debye–Hückel equation is used to calculate activity coefficients, the quality of the fit was independent of the distance parameter, r, and it was set to 8 Å.

Supplementary tables contain the NMR data, including experimental conditions of solvent, temperature, and reactant concentrations for each experiment and the overall rate constants calculated for each sample, on the basis of eq 1 and a modified Bloch equation. Further, tables of conductivity data at 25 °C are given, including concentrations, molar conductivities, and resistance of the pure solvent.

Table IV. Dependence of the Overall Exchange Rate Constants on Reactant Concentrations in Chloroform-d_1 at 20 °C in Order of Decreasing $[Ru(cp)_2I]CF_3SO_3$

$[Ru(cp)_2]$, mM	$[[Ru(cp)_2I]CF_3SO_3]$, mM	$[Ru]_T$, mM	$10^{-3}k$,[a] M^{-1} s^{-1}	$10^{-3}k_{calcd}$, M^{-1} s^{-1}
1.80	9.39	11.19	9.29	7.50
9.13	6.52	15.65	8.29 (8.04)	8.34
18.64	5.22	23.86	8.51	8.94
3.31	5.15	8.46	9.12 (9.03)	8.98
6.11	3.70	9.81	9.74 (10.01)	10.0
9.32	2.61	11.93	10.98	11.3
9.01	2.31	11.32	11.84	11.9
3.05	1.85	4.90	13.05 (13.18)	12.9
13.33	1.43	14.76	13.05	14.2
4.51	1.16	5.67	14.70	15.4
6.66	0.72	7.38	19.02	18.7
5.15	0.56	5.71	21.60	20.7

[a] A second-order rate law is used to calculate observed k's. In the slow-exchange regime the rate constants were determined by using both broadenings of the Ru(II) and Ru(IV) signals according to eq 1.

Table V. Conductivity Data for $[Ru(cp)_2I]CF_3SO_3$ at 25 °C (at μ = 0)

solvent	$K_{ip}°$,[a] M^{-1}	$K_{ip}°$,[b] M^{-1}	$K_{ip}°$,[c] M^{-1}	λ_0,[a] cm^2 mho mol^{-1}	λ_0,[b] cm^2 mho mol^{-1}
$CHCl_3$	4.7×10^6	4.1×10^6	3.8×10^6	12.9	12.2
CH_2Cl_2	5.0×10^4	4.2×10^4	3.4×10^3	30.34	29.50
CH_3CN	2.0	<2.0	9.0	203.1	203.0

[a] Data were fit to Fuoss–Kraus equation. [b] Data were fit to Fuoss–Hsia equation. Solvent dielectric constants and viscosities (cP): $CHCl_3$, 4.7, 0.542; CH_2Cl_2, 8.9, 0.42; CH_3CN, 36.0, 0.345. Distance of closest approach was taken as 8 Å. Estimated error in $K_{ip}°$ ± 25 %. [c] Calculated from eq 2 with r taken as 8 Å.

Discussion

The order of the reaction was studied for the more soluble $Ru(cp)_2/[Ru(cp)_2I]CF_3SO_3$ reaction in $CDCl_3$ (Table IV, supplementary Table 17), CD_2Cl_2, and CD_3CN (both in supplementary Tables 16 and 15, respectively) and was found to be first order in each reactant. Apparent deviations from overall second-order behavior, shown in Table IV, are adequately accounted for by the influence of ion pairing (vide infra). The apparent second-order rate constants presented in Tables I–III were calculated by assuming the simple second-order rate law.

General patterns observed are that the iodine system reacts 2–3 orders of magnitude faster than the bromine system, probably reflecting better bridging and/or conductivity by iodine. Neither system is sensitive to the identity of the anion, but the iodine system

(11) Kirchner, K.; Dodgen, H. W.; Wherland, S.; Hunt, J. P. *Inorg. Chem.* **1989**, *28*, 604.
(12) Harned, H. S.; Owen, B. B. *The Physical Chemistry of Electrolyte Solutions*; Reinhold: New York, 1950.
(13) Fuoss, R. M.; Hsia, K.-L. *Proc. Natl. Acad. Sci. U.S.A.* **1967**, *59*, 1550.
(14) Fernandez-Prini, R. *Trans. Faraday Soc.* **1969**, *65*, 3311.
(15) Beronius, P. *Acta Chem. Scand., Ser. A* **1975**, *A29*, 289.

is more sensitive to the nature of the solvent. The faster iodine system was also studied by using the iodine decamethyl analogue $Ru(C_5Me_5)_2/[Ru(C_5Me_5)_2I]CF_3SO_3$. The lack of measurable reactivity for the decamethyl analogue is in contrast to the outer-sphere electron self-exchange reactions of $Fe(cp)_2/Fe(cp)_2^+$[16] and $Co(cp)_2/Co(cp)_2^+$.[17] In both of these cases, the decamethyl systems are faster, by factors of 3 and 11, respectively, than those of the parent compounds. This has been attributed to increased electron density on the ligand π orbitals involved in electron transfer. The large decrease in rate constant, at least a factor of 10^5, may be partially attributable to the same effect, but here electron density moved from the metal center to the rings will decrease reactivity because the ring π system is not directly involved. A likely more significant contribution may arise from the steric interactions between the methyl groups, which occurs when the (C_5Me_5) rings tilt back in order to form the halogen-bridged precursor.

For more detailed discussion it is useful to treat the higher dielectric constant solvents, CD_3CN, CD_3NO_2, $C_6D_5NO_2$, and C_6H_5CN, separately from the low dielectric ones ($CDCl_3$, CD_2Cl_2, and C_6D_5Br). The conductivity studies (vide infra) established that $[Ru(cp)_2I]CF_3SO_3$ exists as free ions in CD_3CN, and thus it and $[Ru(cp)_2Br]PF_6$ should be fully ionized in all the higher dielectric constant solvents.

The $Ru(cp)_2/[Ru(cp)_2Br]PF_6$ reaction (Table I) showed little if any variation with solvent over the series of high dielectric constant solvents studied. The results for the iodine system, shown in Tables II and III, are rather more varied. The most notable difference is CD_3NO_2, which has a much higher enthalpy and entropy of activation compared to CD_3CN and $C_6D_5NO_2$. No general trend with classical dielectric functions or empirical solvent parameters is found (e.g. $1/\epsilon$[18] or donor/acceptor numbers[19]). This is not surprising, as solvent parameters such as the empirical donor/acceptor numbers are developed for the description of hard–hard Lewis–type interactions and, therefore, should not be applied to interactions where soft reaction centers, such as I or aromatic ring systems, are involved.

In order to interpret the data for the low dielectric constant solvents, the extent of ion pairing must be evaluated. For this purpose, conductivity studies were performed on $[Ru(cp)_2I]CF_3SO_3$. The results are given in Table V. Ion pairing is extensive in both $CHCl_3$ and CH_2Cl_2. This is the result both from the conductivity expressions used in the analysis and from $K_{ip}°$ estimated with eq 2.[20] In these equations, N is Avogadro's number,

$$K_{ip}° = \frac{4\pi Nr^3}{3000}\exp(-w/T) \quad (2a)$$

$$w = \frac{Z_1Z_2e^2}{\epsilon r k_B} \quad (2b)$$

k_B is Boltzmann's constant, r is the distance between the centers of the two ions involved in the ion pair (taken as 8 Å), R is the gas constant, T is the absolute temperature, Z_1 and Z_2 are the charges on the two ions, e is the elementary charge, and ϵ is the dielectric constant.

The values of $K_{ip}°$ for $Ru(cp)_2I^+$ are comparable to the ion-pair formation constants for cobalt(III) clathrochelates in $(CH_2Cl)_2$[21] or manganese(I) isocyanides[22] in chloroform and bromobenzene. There, however, BF_4^- was used as the counterion. It has been reported that, in nonaqueous solvents, triflate is a stronger donor than BF_4^- or PF_6^-.[23]

Table VI. Calculated Second-Order Rate Constants and Ion-Pair Formation Constants (at μ = 0)

solvent (T, °C)	$10^{-5}k_0$, M^{-1} s^{-1}	$10^{-2}k_{ip}$, M^{-1} s^{-1}	$K_{ip}°$,[a] M^{-1}
$CDCl_3$ (20)	7.5 ± 0.4[b]	−2.8 ± 5.9	4.1×10^6
$CDCl_3$ (−20)	3.5 ± 0.6	9.9 ± 9.1	3.6×10^6
CD_2Cl_2 (−50)	2.3 ± 0.5	−0.4 ± 0.5	2.6×10^4
CD_3CN (20)	7.4 ± 0.3[c]		<2
CD_3CN (−30)	0.57 ± 0.02		<2

[a] At temperatures other than 25 °C eq 4 was used to estimate $K_{ip}°$. Solvent dielectric constants: $CHCl_3$, 4.718 (25 °C), 4.806 (20 °C), 5.61 (−20 °C); CH_2Cl_2, 8.9 (25 °C), 12.6 (−50 °C). [b] These estimates of errors are approximately doubled when allowance for uncertainity in $K_{ip}°$ is made. [c] Determined at 20 °C without concentration variation.

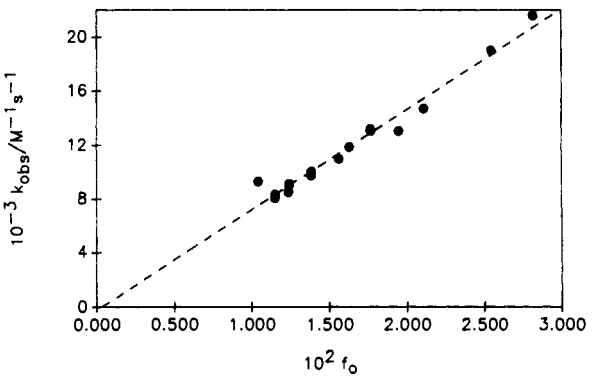

Figure 3. Plot of observed second-order rate constants vs the mole fraction, f_o, of free $[Ru(cp)_2I]^+$. The dashed line was calculated from eq 3.

The existence of both free ions and ion pairs in solution leads to the consideration that they could react independently and could react at different rates.[21-23] The experimental rate constants were fit to eq 3 by using a linear least-squares program. In these

$$k_{exp} = k_0f_0 + k_{ip}f_{ip} = k_0 + (k_{ip} - k_0)f_{ip} \quad (3a)$$

$$\ln \gamma_\pm = -Z_1Z_2C\mu^{1/2}/(1 + Br\mu^{1/2}) \quad (3b)$$

$$\mu = (1 - f_{ip})[Ru(IV)]_0 \quad (3c)$$

$$K_{ip} = K_{ip}°\gamma_\pm^2 \quad (3d)$$

$$K_{ip} = \frac{f_{ip}[Ru(IV)]_0}{(1 - f_{ip})^2[Ru(IV)]_0^2} \quad (3e)$$

equations C and B are the Debye–Hückel parameters and are defined elsewhere,[22] r is the distance of closest approach (taken as 8 Å), $\gamma_\pm$ is the mean activity coefficient, μ is the ionic strength, $K_{ip}°$, is the thermodynamic ion-pair formation constant, and $[Ru(IV)]_0$ represents the total concentration of iodoruthenocene. The fit parameters k_0 and k_{ip}, which are the second-order rate constant of the free-ion pathway and the second-order rate constant of the ion-paired pathway, respectively, are adjusted to minimize χ^2. The rate constants k_0 and k_{ip} were assumed to be independent of ionic strength, since $Ru(cp)_2$ is uncharged. The fraction of free iodoruthenocene, f_0, and ion-paired ruthenocene, f_{ip}, were determined by an iterative procedure using eqs 3b–e. $K_{ip}°$ was taken from the conductance measurements as fit to the Fuoss–Hsia equation.[13]

Since no ion-pair formation constants were availble at temperatures other than 25 °C, $K_{ip}°$ values at other temperatures were estimated by using eq 4, which is derived from eq 2. The values

$$\frac{K_{ip}°(T_2)}{K_{ip}°(T_1)} = \exp\left[(e^2/rk_B)\left(\frac{1}{\epsilon_2T_2} - \frac{1}{\epsilon_1T_1}\right)\right] \quad (4)$$

for $K_{ip}°$ (for μ = 0) and ϵ at different temperatures as well as the

(16) Nielson, R. M.; McManis, G. E.; Golovin, M. N.; Weaver, M. J. *J. Phys. Chem.* **1988**, *92*, 3441.
(17) Nielson, R. M.; McManis, G. E.; Safford, L. K.; Weaver, M. J. *J. Phys. Chem.* **1989**, *93*, 2152.
(18) Born, M. *Z. Phys.* **1920**, *1*, 45.
(19) Schmid, R. *J. Solution Chem.* **1983**, *12*, 135.
(20) Fuoss, R. M. *J. Am. Chem. Soc.* **1958**, *80*, 5059.
(21) (a) Borchardt, D.; Pool, K.; Wherland, S. *Inorg. Chem.* **1982**, *21*, 93. (b) Borchardt, D.; Wherland, S. *Inorg. Chem.* **1984**, *23*, 2537.
(22) Nielson, R. M.; Wherland, S. *Inorg. Chem.* **1984**, *23*, 1338.
(23) Schmid, R.; Kirchner, K.; Dickert, F. L. *Inorg. Chem.* **1989**, *27*, 1530.

calculated second-order rate constants for the free-ion and ion-paired pathway are listed in Table VI. Calculated vs observed second-order rate constants are given in Table IV and are shown in Figure 3.

In outer-sphere electron-transfer reactions between a neutral and a +1 reactant, a small effect of ion pairing has been observed. For the $Fe(cp)_2/Co(cage)_3^{+}$ [21] electron-transfer reaction, k_0/k_{ip} was calculated to be 5.3, 5.6, 19.3, and 19.3 in the solvents CH_3CN, $(CH_3)_2O$, $C_6H_5NO_2$, and $(CH_2Cl)_2$, respectively. For the $Co(cage)_3/Co(cage)_3^{+}$ [24] electron transfer, k_0/k_{ip} was determined to be 3.1, 10, and 5.1 in the solvents CH_3CN, $(CH_3)_2CO$, and $C_6H_5NO_2$, respectively. In contrast, for the $Ru(cp)_2/Ru(cp)_2I^+$ reaction, the rate constant for the ion-paired pathway is negligibly small, i.e. at least smaller by a factor of 10^5. A plot of the observed second-order rate constants vs the fraction, f_0, of the free iodoruthenocene is linear with an intercept ($=k_{ip}$) of $(-2.8 \pm 5.9) \times 10^2$ M^{-1} s^{-1} and a slope ($=k_0$) of $(7.5 \pm 0.4) \times 10^5$ M^{-1} s^{-1} (Figure 3). It is, therefore, assumed that the triflate ion is coordinated in the vicinity or even at the iodine site, preventing the formation of a bridged precursor complex. The rate constants for the free-ion pathway in chloroform and methylene chloride are comparable to the rate constants for the high dielectric constant solvents. $\Delta H^{\ddagger}$ and $\Delta S^{\ddagger}$ for this pathway in chloroform are calculated to be 2.8 ± 1.7 kcal mol^{-1} and -22 ± 7 cal mol^{-1} K^{-1}, respectively, which are comparable to the values given in Table II for the observed rate constants. According to eq 4, ΔH° and ΔS° are 0.4 kcal mol^{-1} and 29 cal mol^{-1} K^{-1}, respectively, for ion-pair formation in $CHCl_3$. This prediction is in line with other experimental data.[25-27]

Since low dielectric constant solvents are poorer donor/acceptor solvents than high dielectric constant, ones,[19] in general one can expect a lower $\Delta H^{\ddagger}$ of desolvation and a somewhat more negative $\Delta S^{\ddagger}$, as less entropy is gained on release of the poorer solvent. This is, qualitatively, in line with the experimental data, as can be seen in Tables II and III.

An interesting and perhaps unusual temperature dependence of the line widths of $Ru(cp)_2I^+$ has been observed in some batches. Since the effect is abolished by I_2, which can act as an oxidant, some reducing species is indicated. Perhaps some Ru(III) species appears as the temperature is increased. The paramagnetic Ru(III) species could produce some line broadening and the small shifts observed. Since the effect seems to be reversible, either a disproportionation equilibrium or an equilibrium with an oxidized solvent or impurity species appears to be required. Electron spin resonance studies have not revealed any evidence for Ru(III), but this fact does not conclusively rule out Ru(III) since in low-spin 17-electron metallocenes significant orbital contributions to the magnetic moment are expected, which lead to fast electronic relaxation, and EPR spectra can be typically observed only at very low temperatures.[28] Due to the lack of a significant chemical shift, which indicates a reaction in the "slow exchange" regime, the presence of Ru(II) in our solutions can be excluded, since no Ru(II) signal could be detected by NMR spectroscopy. A monomeric or dimeric haloruthenocene(III) compound with halide coordinated might be stable, since it is known that transition-metal metallocenes with only partially filled orbitals relieve their electron deficiency by adding extra ligands, accompanied by a tilted-back arrangement of cyclopentadienyl rings. In view of the sparse information to date, a more detailed investigation has to be done.

In conclusion, this study has characterized the electron-transfer reaction between $Ru(cp)_2$ and $Ru(cp)_2X^+$ in various solvents through its activation parameters and rate constants. In low dielectric constant solvents, as expected, ion pairing occurs, which in general makes it difficult to determine specific rate constants and activation parameters. In accordance with outer-sphere electron-transfer reactions of the same charge type, the ion-paired pathway is less favorable. However, in the case of these particular inner-sphere electron-exchange processes, the inhibition due to ion pairing is much more pronounced and the ion-paired pathway is practically negligible. This finding suggests that the triflate ion must be coordinated at the halogen or at least in the vicinity of the bridging ligand, obstructing precursor complex formation. Further investigations will involve temperature-dependent conductance measurements and concentration dependence studies at various temperatures in order to separate k_0 and k_{ip} from the apparent k and to get activation parameters for both pathways. The activation parameters for the $Ru(cp)/Ru(cp)_2I^+$ system have proven to be more varied than those for the $Ru(cp)_2/Ru(cp)_2Br^+$ system. Specific solvent interactions with the iodine might be involved. Our results are consistent with those of Taube et al.[5], considering the precision of the activation parameters. The haloruthenium system cannot easily use an outer-sphere mechanism such as is presumed in the ferrocene/ferrocenium[29] case. Apparently the Br bridge for ruthenium is not as efficient as the outer-sphere ring interaction for iron, as a larger $\Delta H^{\ddagger}$ is found for ruthenium. The iodoruthenium parameters are closer to those of the outer-sphere iron systems. Further work will also involve the study of the volume of activation as a function of solvent and halogen ligand in order to better interpret the results. An extension of these studies to the osmium analogues is in progress.

It might be noted that $\Delta V^{\ddagger}$ for ferrocene/ferrocenium is ca. -7 cm^3 mol^{-1} [29] and for bromoruthenocene(IV) is ca. -3 cm^3 mol^{-1}.[11] In both cases the larger negative $\Delta V^{\ddagger}$ contribution expected for association or bond formation is largely compensated for by a positive $\Delta V^{\ddagger}$ effect due to solvent release on association.

Note Added in Proof. In work on the Os analogues of these Ru compounds, we find that the non-ion-pair, ion-pair pathway treatment does not fit the data. Both the Ru and Os data can be fit with the rate law

$$\text{rate} = k_0[\text{M(II)}] + k_1[\text{M(II)}][\text{M(IV)}]$$

Acknowledgment. We acknowledge the assistance of Don Appel with the NMR measurements. This work is supported by the National Science Foundation and by the Boeing Co. through funds for the purchase of the Nicolet instrument. We also thank Dr. L. F. Han and Prof. R. Schmid (Technical University of Vienna) for performing the conductance measurements.

Supplementary Material Available: Tables of observed second-order rate constants as a function of temperature and solvent and conductance data for $[Ru(cp)_2I]CF_3SO_3$ in chloroform, methylene chloride, and acetonitrile (11 pages). Ordering information is given on any current masthead page.

(24) Gribble, J.; Wherland, S. *Inorg. Chem.* **1989**, *28*, 2859.
(25) Bien, G. S.; Kraus, C. A.; Fuoss, R. M. *J. Am. Chem. Soc.* **1934**, *56*, 1860.
(26) Carrajal, C.; Tolle, K. J.; Smid, J.; Szwarc, M. *J. Am. Chem. Soc.* **1965**, *87*, 5548.
(27) Sears, P. G.; Wilhoit, E. G.; Dawson, L. R. *J. Phys. Chem.* **1956**, *60*, 169.
(28) O'Hare, D.; Green, J. C.; Chadwick, T. P.; Miller, J. S. *Organometallics* **1988**, *7*, 1335.
(29) Kirchner, K.; Dang, S. Q.; Stebler, M.; Dodgen, H. W.; Wherland, S.; Hunt, J. P. *Inorg. Chem.* **1989**, *28*, 3605.